Acta Geodyn. Geomater., Vol. 20, No. 2 (210), 71–82, 2023
DOI: 10.13168/AGG.2023.0007
journal homepage: https://www.irsm.cas.cz/acta

ORIGINAL PAPER

A NEW ADAPTIVE WVS BASED DENOISING METHOD ON GNSS VERTICAL TIME SERIES

Zhengkai HUANG [1], Zengnan HOU [1], Jiahui HUANG [2], Xiwen SUN [3], Xiaoxing HE [2] *, Hongkang CHEN [3] and Jean-Philippe MONTILLET [4]

[1] *School of Transportation Engineering, East China Jiao Tong University, Nanchang 330013, China*
[2] *School of Civil and Surveying and Mapping Engineering, Jiangxi University of Science and Technology, Ganzhou 341000, China*
[3] *School of Surveying and Geoinformation Engineering, East China University of Technology, Nanchang 330013, China*
[4] *Space and Earth Geodetic Analysis Laboratory, University of Beira Interior, Covilhã, Portugal*

**Corresponding author's e-mail:* xxh@jxust.edu.cn

ARTICLE INFO

Article history:
Received 5 May 2023
Accepted 20 June 2023
Available 26 June 2023

Keywords:
Whale Optimization Algorithm
Variational Mode Decomposition
Singular Spectrum Analysis
Empirical Mode Decomposition
Ensemble Empirical Mode Decomposition

ABSTRACT

Improper selection of modal decomposition numbers and penalty factors in Variational Modal Decomposition (VMD) can result in over-decomposition and under-decomposition issues, impacting the analysis of high-precision Global Navigation Satellite System (GNSS) time series for geodynamics and geophysics research purposes. This work shows a new WOA-VMD-SSA (WVS) denoising method combining Whale Optimization Algorithm (WOA) and the VMD together with the Singular Spectrum Analysis (SSA) method. Simulated data comprising a combination of Flicker noise plus White noise (FN+WN) and General Gauss-Markov plus White noise (GGM+WN) were utilized in our experiments. That the simulation results show that WVS root mean square error (RMSE) decreased by 0.88 to 0.91mm compared to Empirical Mode Decomposition (EMD), Ensemble Empirical Mode Decomposition (EEMD) and Complete Ensemble Empirical Mode Decomposition with Adaptive Noise (CEEMDAN). The signal-to-noise ratio (SNR) and correlation coefficient (CC) increased by 1.08 to 1.12 dB and 0.17 to 0.18, respectively. And the WVS method has the smallest difference from the true value. Finally, experimental analysis was conducted by using the vertical component of the GNSS time series from 100 GNSS sites located in the west coast of the USA. The real data results show that compared with EMD, EEMD and CEEMDAN methods, WVS can effectively reduce the uncertainty of station velocity and obtain more accurate velocity values, which is consistent with the conclusions of our simulations. Besides, the WVS algorithm can adaptively determine the optimal parameters for VMD decomposition, and it is also more efficient in time series noise removal.

1. INTRODUCTION

With the rapid development of space observation technologies, the International GNSS Service (IGS) reference stations worldwide have accumulated more than 20 years of data (Shen et al., 2019; Bock and Melgar, 2016; He et al., 2020), providing important data support for studying crustal deformation and plate tectonic motions (Fernandes et al., 2004; Serpelloni et al., 2013; Montillet et al., 2015; He et al., 2017). However, due to various factors, e.g., multipath effects, clock errors, tropospheric delays, the GNSS time series contain complex noise (i.e., coloured and white noises), and exhibits nonlinear changes (e.g., post-seismic relaxation), which impact on the estimation of GNSS station velocity (Tregoning and Watson., 2009; Han et al., 2006). Therefore, reducing the amplitude of the noise in GNSS time series is of great significance for the research and analysis of GNSS time series.

For the denoising of GNSS time series, a Kalman filter can be used to estimate the position, velocity, and clock bias of a receiver, and to reduce the effects of signal errors and noise. It is a recursive filter that continually updates the estimate and covariance matrix in order to adapt to changing environmental and noise conditions. However, in case of a high amplitude noise or an inaccurate model, this filter may not effectively remove the noise (Meinhold and Singpurwalla, 1983). The wavelet packet decomposition denoising algorithm proposed by Mosavi et al. (2017) is a signal denoising method based on wavelet transforms. The basic functions of wavelet packet decomposition have good locality in time and frequency, which can better capture local features and details of the signal. However, threshold processing may filter out small details in the signal, which may lead to the loss of some important information (Yen and Lin, 2000; Mosavi et al., 2017; El-Hendawi and Wang, 2020).

Singular Spectrum Analysis (SSA) is a signal analysis and denoising method based on matrix decomposition. It has good ability to capture short-term changes, and the algorithm can process linear and nonlinear signals (Elad and Aharon, 2006; Alexandrov, 2008). However, it has high computational complexity, and the number of

Cite this article as: Huang Z, Hou Z, Huang J, Sun X, He X, Chen H, Montillet J-P: A new adaptive WVS based denoising method on GNSS vertical time series denoising. Acta Geodyn. Geomater., 19, No. 2 (210), 71–82, 2023. DOI: 10.13168/AGG.2023.0007

eigenfunctions obtained from the decomposition may be more than the actual number of eigenfunctions in the signal, requiring further processing based on the actual situation (Vautard et al.,1992).

The Empirical Mode Decomposition (EMD) algorithm proposed by Huang et al. (1998) is suitable for processing nonlinear and non-stationary signals, and it is an adaptive denoising algorithm. But it has endpoint effects and mode mixing problems (Huang et al.,1998; Montillet et al., 2012). To address the mode mixing problem of the EMD algorithm, Huang et al. (2009) proposed the Ensemble Empirical Mode Decomposition (EEMD) algorithm and the Complementary Ensemble Empirical Mode Decomposition (CEEMD) algorithm. By adding white noise to the signal to be decomposed before the EMD decomposition, the mode mixing problem in the EMD decomposition is efficiently suppressed. Both algorithms can handle different types of signals, making them suitable for denoising nonlinear and non-stationary signals. However, there may be large errors when decomposing low-frequency signals (Wu et al., 2009; Lei et al., 2009; Jiang et al., 2013; Wang et al., 2015; Agnieszka and Dawid, 2022; Li et al., 2015; Liu et al., 2020). The Complete Ensemble Empirical Mode Decomposition with Adaptive Noise (CEEMDAN) algorithm decomposes the original signal into a series of Intrinsic Mode Functions (IMFs), and performs multiple decompositions on each IMF to form multiple sets of IMFs. The final decomposition result is obtained by averaging these IMFs, avoids the problem of the misalignment of the final ensemble average caused by the differences in the decomposition in IMFs (Xiao et al., 2018; Xiong et al., 2019). However, it requires in general a large amount of processing time (Dey et al., 2021; Wang et al., 2021).

The Variational Mode Decomposition (VMD) algorithm was proposed by Dragomiretskiy and Zosso (2013). The VMD method avoids the mode mixing problem and has better computational efficiency, and is widely used in signal denoising research. It simplifies the process of mode decomposition and exhibits excellent separation performance. However, the VMD algorithm requires manually setting the parameters. When the number of decompositions (k) and the penalty factor (α) are not selected properly, the noise reduction cannot be effectively achieved (Humphrey et al., 1996; Zhang et al., 2018; Zhang et al., 2020). Here, we use the Whale Optimization Algorithm (WOA) proposed by Mirjalili and Lewis (2016), with the minimum envelope entropy as the fitness function to obtain the optimal parameter combination for the VMD decomposition. However, how can we efficiently integrate multiple algorithms to denoise efficiently the GNSS time series signals need further investigation.

To solve these problems, A WOA-VMD-SSA(WVS) method is proposed here we use the WOA optimization algorithm to determine the optimal parameter combination (k, α) of the VMD algorithm. An improved method for secondary denoising of the SSA algorithm based on comprehensive evaluation indicators is adopted. It helps with studying crustal movement, deformation, and plate tectonic motion. The remaining sections of this paper are organized as follows: Section 2 introduces the background theory of VMD, SSA and the flowchart of the WVS algorithm. Section 3 verifies the WVS method by simulating time series with random noise and analyzes the up component of the time series for 100 sites located along the west coast of the USA. Section 4 concludes our study.

2. PRINCIPLE AND METHOD

2.1. VARIATIONAL MODE DECOMPOSITION

The VMD decomposition considers that each signal is composed of several IMFs with specific center frequencies and limited bandwidths. It is a process of constructing and solving a constrained variational problem. The variational model is such as (Humphrey et al., 1996; Jin et al., 2022):

$$\begin{cases} \min\limits_{\{\mathrm{uk}\},\{\omega k\}} \left\{ \sum\limits_{k} \left\| \partial_t \left[\left(\delta(t) + \frac{j}{\pi t} \right) * u_k(t) \right] e^{-j\omega_k t} \right\|_2^2 \right\} \\ s..t. \sum\limits_{k} u_k = f \end{cases} \tag{1}$$

In the equation, $\{u_k\} = \{u_1, u_2, \cdots u_k\}$ are the k modal components, $\{\omega_k\} = \{\omega_1, \omega_2, \cdots \omega_k\}$ are the frequencies corresponding to the k modal components, $\delta(t)$ is the pulse function, and f is the input signal.

By introducing the second-order penalty factor α and the Lagrange multiplier $\lambda(t)$, Equation (1) can be transformed into an unconstrained variational problem. The obtained extended Lagrangian expression is (Humphrey et al., 1996; Xu et al., 2021):

$$L(\{u_k\},\{\omega_k\},\lambda) = \alpha \sum_k \left|\left| \partial_t \left[\left(\delta(t) + + \frac{j}{\pi t} \right) * u_k(t) \right] e^{-j\omega_k t} \right|\right|_2^2 + \left|\left| f(t) - \sum_k u_k(t) \right|\right|_2^2 + + \langle \lambda(t), f(t) - \sum_k u_k(t) \rangle \tag{2}$$

Where α is the penalty factor, and $\lambda(t)$ is the Lagrange multiplier. Using the Alternating Direction Method of Multipliers (ADMM), continuously alternating the updates of $\hat{u}_k^{n+1}$, ω_k^{n+1} and $\hat{\lambda}^{n+1}$ to obtain the optimal value of Equation (2).

$$\mu_k^{n+1}(\omega) = \frac{\hat{f}(\omega) - \sum_{i \neq k} \hat{\mu}_i(\omega) + \hat{\lambda}(\omega)/2}{1 + 2\alpha(\omega - \omega_k)^2} \tag{3}$$

$$\omega_k^{n+1} = \frac{\int_0^\infty \omega \left| \hat{\mu}_k^{n+1}(\omega) \right|^2 d\omega}{\int_0^\infty \left| \hat{\mu}_k^{n+1}(\omega) \right|^2 d\omega} \tag{4}$$

$$\hat{\lambda}^{n+1}(\omega) = \hat{\lambda}^n(\omega) + \tau \left(f(\omega) - \sum_{k=1}^{k} \hat{\mu}_k^{n+1}(\omega) \right) \tag{5}$$

Where $\hat{f}(\omega)$, $\hat{\mu}_k(\omega)$, $\hat{\mu}_k^{n+1}(\omega)$ and $\hat{\lambda}(\omega)$ represent the Fourier transforms of $\hat{f}(t)$, $\hat{\mu}_k(t)$, $\hat{\mu}_k^{n+1}(t)$, $\lambda(t)$, n is the number of iterations, τ is the iteration step size.

When Equation (6) is satisfied, the iteration ends and the N_i (i=1...k) IMF components are obtained, where ε is the convergence tolerance (ε>0).

$$\sum_{i=1}^{k} \frac{\|\hat{u}_i^{n+1} - \hat{u}_i^n\|_2^2}{\|\hat{u}_i^n\|_2^2} < \varepsilon \tag{6}$$

2.2. SINGULAR SPECTRUM ANALYSIS

SSA is a method for studying and analyzing the nonlinear signals. It first selects $(1, N/2)$ window length M within the interval a and constructs an $N * M$ trajectory matrix for the time series of length N. The construction is in the form of Equations (7) and (8) (Vautard et al., 1992).

Original time series:

$$x_i = [x_1 \quad x_2 \quad \cdots \quad x_N] \tag{7}$$

Trajectory matrix:

$$X_{MN} = [x_1 \quad x_2 \quad \cdots \quad x_N] = \begin{bmatrix} x_1 & x_2 & \cdots & x_{N-M+1} \\ x_2 & x_3 & \cdots & x_{N-M+2} \\ \vdots & \vdots & \ddots & \vdots \\ x_M & x_{M+1} & \cdots & x_{MN} \end{bmatrix} \tag{8}$$

where z is defined as:

$$Z = N - M + 1 \tag{9}$$

Subsequently, the eigenvalues and eigenvectors of the trajectory matrix are estimated by diagonalizing the matrix, and arranging the diagonal elements in descending order. Determining the components of the time series for reconstruction. The reconstruction formula is shown in Equation (10).

$$y_i = \begin{cases} \frac{1}{i}\sum_{M=1}^{Z} X_{M,i-M+1}^{1 \le i \le M} \\ \frac{1}{M}\sum_{M=1}^{L} x_{M,i-M+1}^{M \le i \le Z} \\ \frac{1}{N-i+1}\sum_{M-1-Z+1}^{N-Z+1} x_{M,i-M+1}^{Z \le i \le N} \end{cases} \tag{10}$$

where y_i represents the reconstituted time series after grouping. $x_{M,i-M+1}$ is the reconstituted time series. N is the length of the time series. M is the window length, and Z is $N - M + 1$.

2.3. WOA-VMD-SSA

The WOA algorithm is an optimization algorithm based on the social behavior of whales. It achieves optimization by simulating the feeding behavior of whale. The basic idea is to transform optimization problems into the process of finding the optimal solution in the search space. The algorithm initializes by randomly generating a certain number of candidate solutions as the initial whale population. Each candidate solution is referred to as one whale. Next, the whale will move and adjust its position according to its position and fitness value (Mirjalili and Lewis, 2016).

Here, the envelope entropy function is selected as the fitness function for optimizing VMD parameters using the WOA algorithm. The envelope entropy represents the sparse characteristics of the original signal. When there is more noise in the IMF, the envelope entropy value is larger, and vice versa. The principle of envelope entropy is shown in Equation (11) (Jin et al., 2022).

$$\begin{cases} Ep = -\sum_{j=1}^{N} pj \, lg \, p \, j \\ Pj = a(j) / \sum_{j=1}^{N} a(j) \end{cases} \tag{11}$$

where $a(j)$ is the envelope signal of the k modal components obtained by Hilbert demodulation of VMD decomposition; P_j is the normalization of $a(j)$; N is the number of sampling points. The Hilbert formula (12) is as follows.

$$a(j) = x(t) * \frac{1}{\pi * t} \tag{12}$$

where x(t) represents the k modal components obtained from the VMD decomposition.

For the high-frequency noise obtained after VMD decomposition, the SSA algorithm with a comprehensive evaluation index as the classification index will be used for secondary denoising to improve the denoising effect. The specific process of the WVS denoising method is as follows, flowchart of WVS method as shown in Figure 1.

Step1: Set the VMD parameter range and WOA algorithm initialization parameters. In the experimental process, Select separately $k \in (2.10)$, $k \in (2.15)$, $k \in (2.20)$ and $\alpha \in (10.5000)$, $\alpha \in (10,10000)$. To ensure the completeness of signal decomposition in the experiment, this article selects $k \in (2.20)$, $\alpha \in (10.10000)$ as the VMD parameter range. The best search proxy number n for WOA is 30, and the number of iterations L of optimal convergence value is 10 (Xu et al., 2021). Half the length of the time series to be denoised is used as the SSA window length (Hassani et al., 2011).

Step2: Use the WOA optimization algorithm with the minimum value of envelope entropy as the fitness function to calculate the optimal number of modes *k* and the penalty factor α, and use the optimal parameters for time series VMD decomposition.

Step3: Reconstruct the time series by sequentially summing each IMF decomposed by VMD, and calculate the T (comprehensive evaluation index) for each reconstructed time series. When the T value is the smallest, the corresponding reconstructed time series is the denoised time series, and the remaining IMF components are regarded as high-frequency noise.

Step4: The high-frequency noise in step 3 is further denoised by SSA. The SSA decomposition results are classified by comprehensive evaluation indexes, extracting denoising time series, and combined with the denoising time series in step 3 to form the final denoising time series.

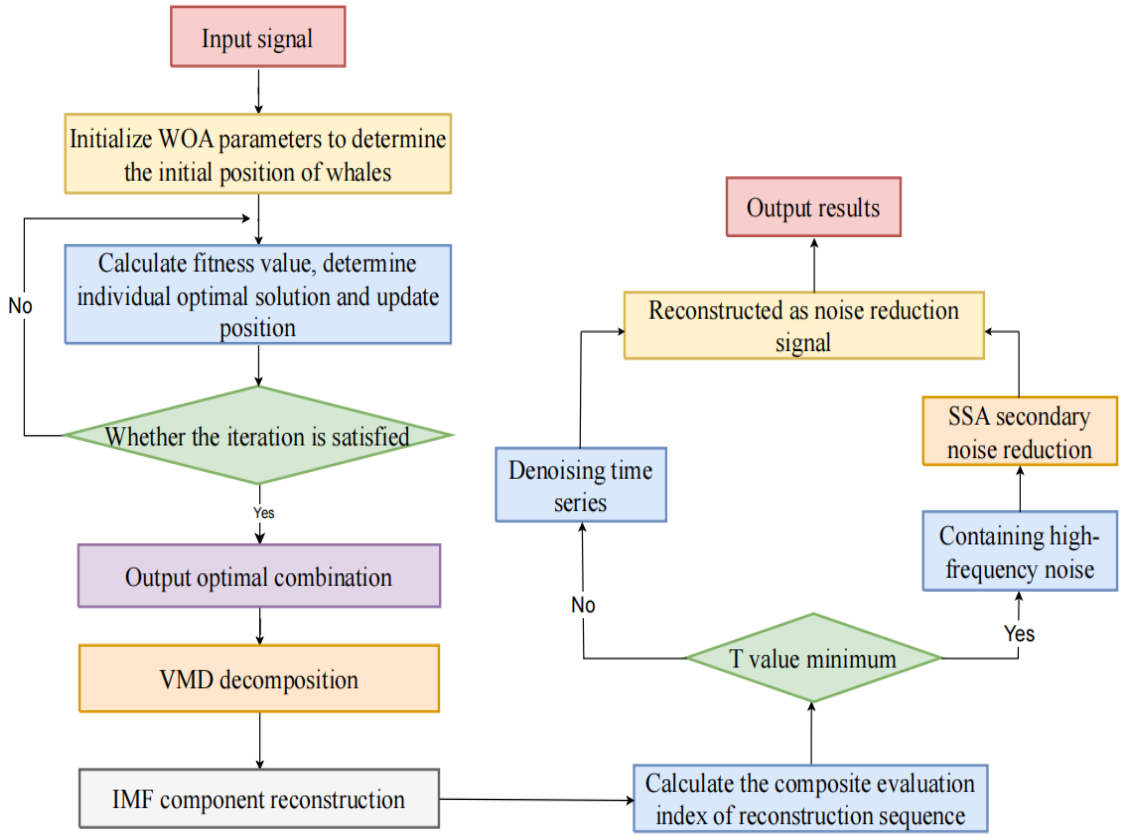

Fig. 1 Flowchart of WVS method.

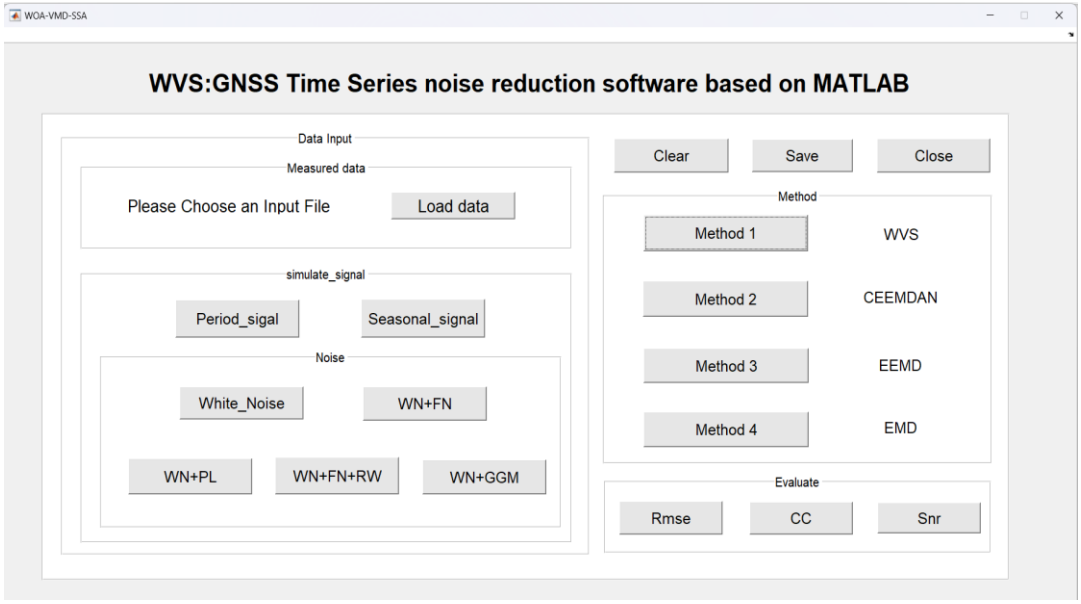

Fig. 2 WVS software design interface.

3. EXPERIMENT ANALYSIS AND DISCUSSION

3.1. DESIGN OF WVS SOFTWARE ON GNSS TIME SERIES NOISE REDUCTION

To implement the WVS denoising method described in the previous section 2.3, a noise reduction software based on MATLAB named WVS was designed for the denoising method proposed in the previous section. The main interface of the software is shown in Figure 2. The software can be launched by running "WOA-VMD-SSA.m". The software includes four modules: data import, denoising processing, data plots and result analysis. Data import module includes the import of simulation data and station measured data. The simulated data includes time-varying signal simulation with colored noise and periodic signal simulation with colored noise. The denoising processing module provides four methods: WVS, CEEMDAN, EEMD and EMD. Result analysis

Table 1 Parameters of the simulated GNSS time series.

Site	Driving Noise	Fraction FN/GGM	Fraction WN	value of d	1-phi
FNWN	2.3	0.95 (FN)	0.05	-	-
GGMWN	2.3	0.99 (GGM)	0.01	0.75	0.03

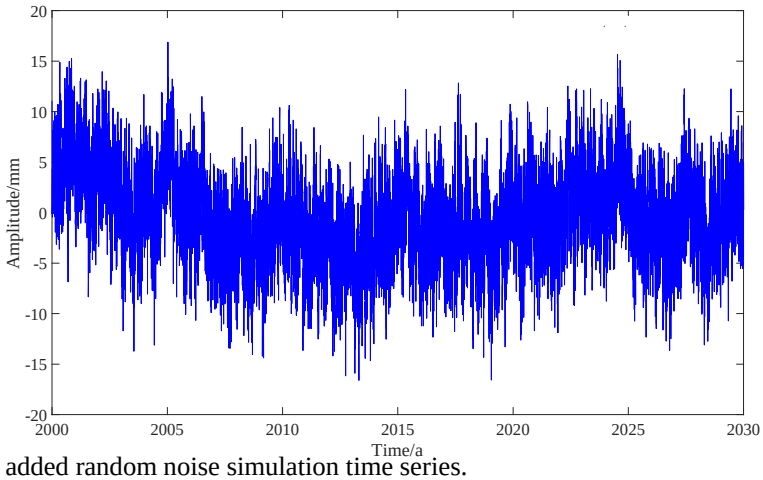

Fig. 3 FNWN with added random noise simulation time series.

module evaluates the denoising results using root mean square error (RMSE), correlation coefficient (CC) and signal-to-noise ratio (SNR) as evaluation indicators. RMSE is a commonly used method for measuring the error between data before and after denoising. The smaller the value, the better the denoising effect. CC indicates the degree of the relationship between data before and after denoising and the higher the value, the better the preservation of the basic characteristics of the data. SNR is the ratio of the signal strength to the noise strength and can be used to evaluate the clarity and reliability of the signal. The higher the value, the less noise it contains. Based on the developed software, the effectiveness of the WVS method for denoising time series signals was validated using simulated data with colored noise added to a time-varying signal and a periodic signal together with real GNSS times, for details see in later section 3.2.

3.2. DENOISING ANALYSIS OF SIMULATED GNSS TIME SERIES

Many scholars believe that FNWN and GGMWN noise models are the optimal noise models for GNSS vertical coordinate time series. Therefore, we chose FNWN and GGMWN stochastic noise models in our simulations (Williams et al., 2004). Each time series are generated using the Hector software (Bos et al., 2013; He et al., 2017) with parameters specified in Table 1 for the Flicker Noise + White Noise (FN+WN) and General Gauss-Markov + White Noise (GGM+WN) models. In addition, a random noise is added to the simulated time series. The WVS software is used to import the station data and the EMD, EEMD, CEEMDAN and WVS methods are applied to the simulated data. An example of simulated time series is shown in Figure 3.

The optimal parameters of the VMD decomposition can be obtained through the algorithm results, which are k = 9 and α = 3670. The simulated FNWN time series is decomposed using the VMD algorithm with this optimal parameter combination. The results are shown in Figure 4 using the simulated time series in Figure 3.

Figure 4 displays the 9 IMFs from the VMD decomposition. In order to extract any useful signal and determine the boundary between high-frequency and low-frequency signals in the IMF components, the 9 IMFs are sequentially added together and reconstructed. The comprehensive evaluation indicators are used to calculate the indicator values T of the reconstructed time series. The statistical results are shown in Table 2.

Table 2 Comprehensive evaluation indicator results.

	Reconstruct time series								
Index	$\sum_{i=1}^{9} IMFi$	$\sum_{i=2}^{9} IMFi$	$\sum_{i=3}^{9} IMFi$	$\sum_{i=4}^{9} IMFi$	$\sum_{i=5}^{9} IMFi$	$\sum_{i=6}^{9} IMFi$	$\sum_{i=7}^{9} IMFi$	$\sum_{i=8}^{9} IMFi$	$\sum_{i=9}^{9} IMFi$
T	0.36	0.30	0.28	0.27	0.28	0.33	0.40	0.52	0.64

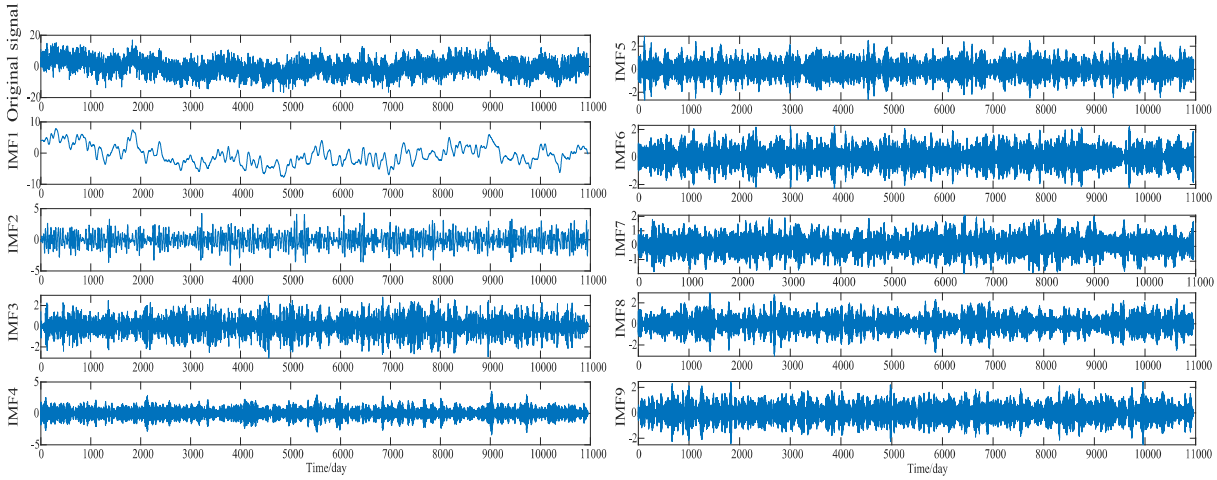

Fig. 4 VMD decomposition results of simulated FNWN time series.

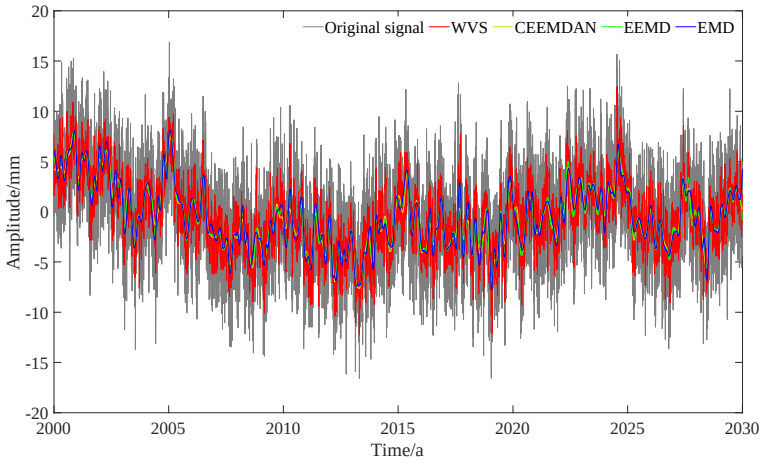

Fig. 5 Simulation data noise reduction comparison results.

From Table 2, it can be seen that for i=4 the minimum value of 0.27 is reached. Therefore, it is considered that IMF5-IMF9 are associated with the high-frequency noise. The SSA algorithm is used to further denoise the time series. The signal is classified by using the comprehensive evaluation index after SSA algorithm decomposition, and the (useful) signal is extracted and combined with the reconstructed time series using IMF1-IMF4. The EMD, EEMD and CEEMDAN methods are also used for comparison with the proposed method, Figure 5 displays the results with all the algorithms. Due to the fact that the real signal is known, it allows to estimate the difference between the results from the algorithms (EMD, EEMD, CEEMDAN, WVS) and the true value using three indicators (i.e. RMSE, SNR, CC). The statistical results are shown in Table 3.

Figure 5 and Table 3 show that the WVS method has a better fitting effect and retained more useful signals compared to EMD, EEMD and CEEMDAN methods. The RMSE is reduced by 0.91 mm, 0.88 mm, 0.91 mm, respectively. The SNR increases by 1.12 db, 1.08 db, 1.08 db, respectively. The CC also increases by 0.18, 0.17, 0.18, respectively. The small RMSE indicates that the extracted signal closer to the real simulated signal. The SNR can reflect the proportion of signal to noise. A high SNR indicates better denoising effect. The CC can measure the linear relationship between the extracted signal and the simulated time series. A high CC indicates a strong similarity between the denoised signal and the real signal. We conclude that the noises reduction effect of the WVS method is better than that of EMD, EEMD and CEEMDAN methods. Furthermore, this study uses Hector software (Bos et al., 2013) to calculate the velocity and velocity uncertainty of simulated data and denoised data with added random noise under the FNWN and GGMWN noise models to further verify the effectiveness of the WVS algorithm. The velocity values of the denoised data and simulated data are shown in Figure 6. The statistical results of the difference between the velocity uncertainty values after denoising and the true velocity uncertainty values are shown in Figure 7.

Table 3 Comparison between the accuracy evaluation index results of simulation data denoising results and actual values.

Method	***diff*_RMSE (mm)**	***diff_SNR* (db)**	***diff_CC***
WVS	0.19	-0.80	-0.02
CEEMDAN	1.10	-1.92	-0.20
EEMD	1.07	-1.88	-0.19
EMD	1.10	-1.88	-0.20

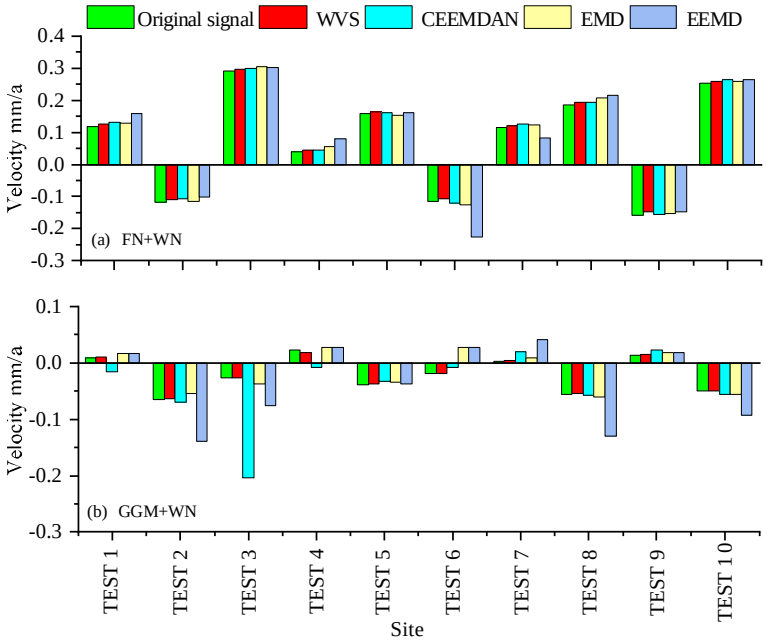

Fig. 6 Comparison results of velocity after noise reduction in WVS/CEEMDAN/EEMD/EMD simulation data.

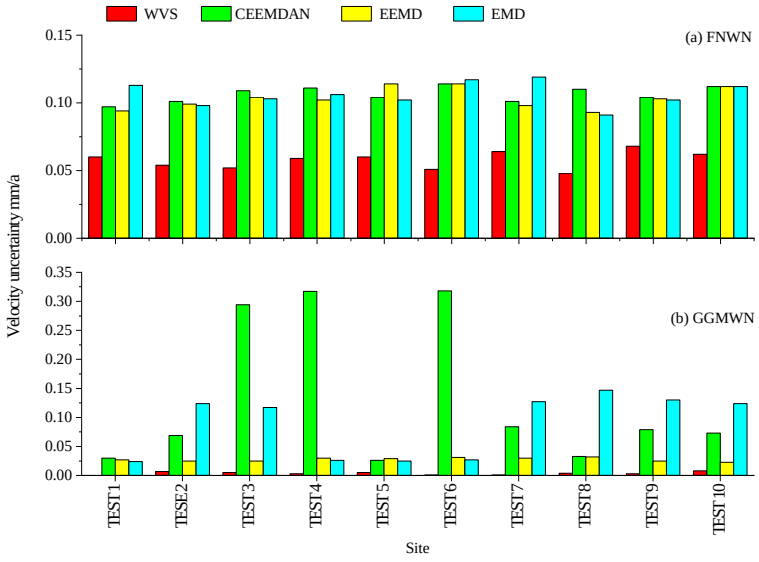

Fig. 7 Comparison results of velocity uncertainty after noise reduction in WVS/CEEMDAN/EEMD/EMD simulation data.

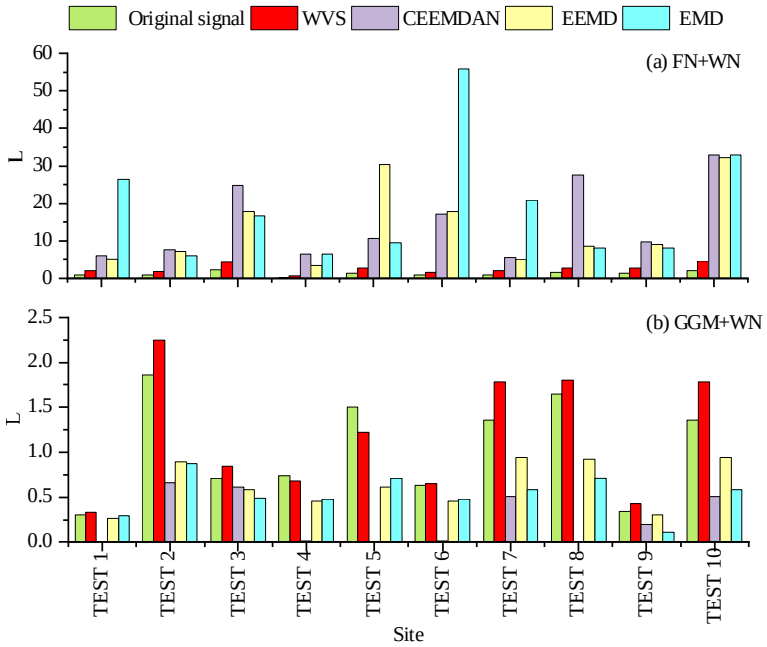

Fig. 8 Comparing the results using the ratio L after noise reduction applying the WVS, CEEMDAN, EEMD,

Figures 6 and 7 show the WVS results comparing with the other three denoising methods. WVS is the closest to the true value of velocity and velocity uncertainty under FNWN and GGMWN model estimation. This indicates that the WVS method can maintain the integrity of the original model (i.e. stochastic noise properties). However, CEEMDAN method has poor removal effect on FNWN and GGMWN colored noise.

In addition, the velocity uncertainty value can reflect the absolute error in the station velocity, while the ratio L of station velocity to velocity uncertainty reflects its relative error: a large ratio means small confidence in estimate (Montillet et al., 2015). Finally, the velocity/ (velocity uncertainty) ratio L of the real signal is compared with the ratio L estimated by the four denoising methods, as an experimental reference for the measured data. The results with the ratio L are shown in Figure 8. Under the FNWN and GGMWN models, the denoised ratio L of the WVS method is closer to the real signal ratio L than other methods. This shows that the velocity and velocity uncertainty results obtained by the denoising WVS method are the most reliable.

3.3. APPLICATION OF WVS FOR GNSS TIME SERIES DENOISING ANALYSIS.

We now analyze the daily time series from the Extended Solid Earth Science ESDR System (WNAM_Clean_TrendNeuTimeSeries_comb.zip, Bock et al., 2021). The distribution of the selected 100 GNSS sites is shown in Figure 9. Select the vertical direction time series with time interval 2008-2022. The EMD, EEMD, CEEMDAN and WVS methods are then applied. The parameter settings for the algorithm are the same as those in the simulations.

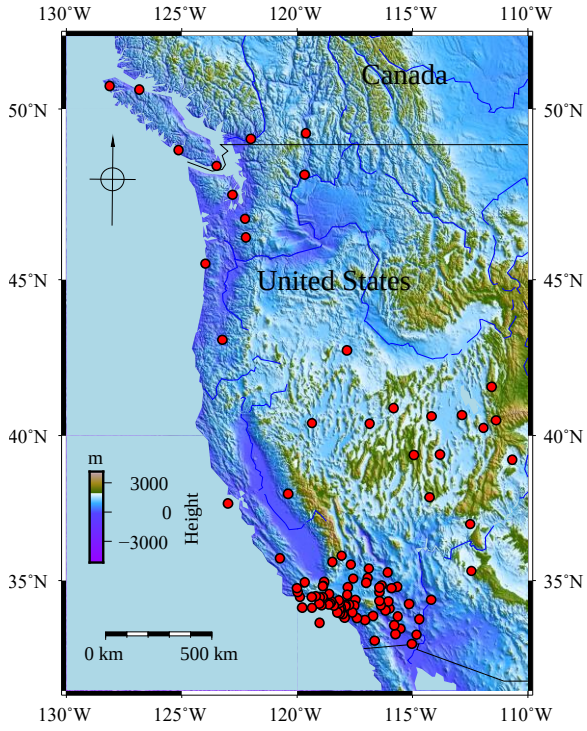

Fig. 9 Spatial distribution of the analyzed 100 GNSS sites.

Due to the unknown true signal for each site, the RMSE, SNR and CC cannot be used as indicators to evaluate the time series noise reduction. Therefore, we rely on the ratio L defined in the previous section (Montillet et al., 2015), as using the Hector software, we calculate the estimated velocity uncertainty values before and after noise reduction using the previous selected stochastic noise models (i.e. FNWN and GGMWN), and conduct statistical comparative analysis. The statistical results are shown in Figure 10.

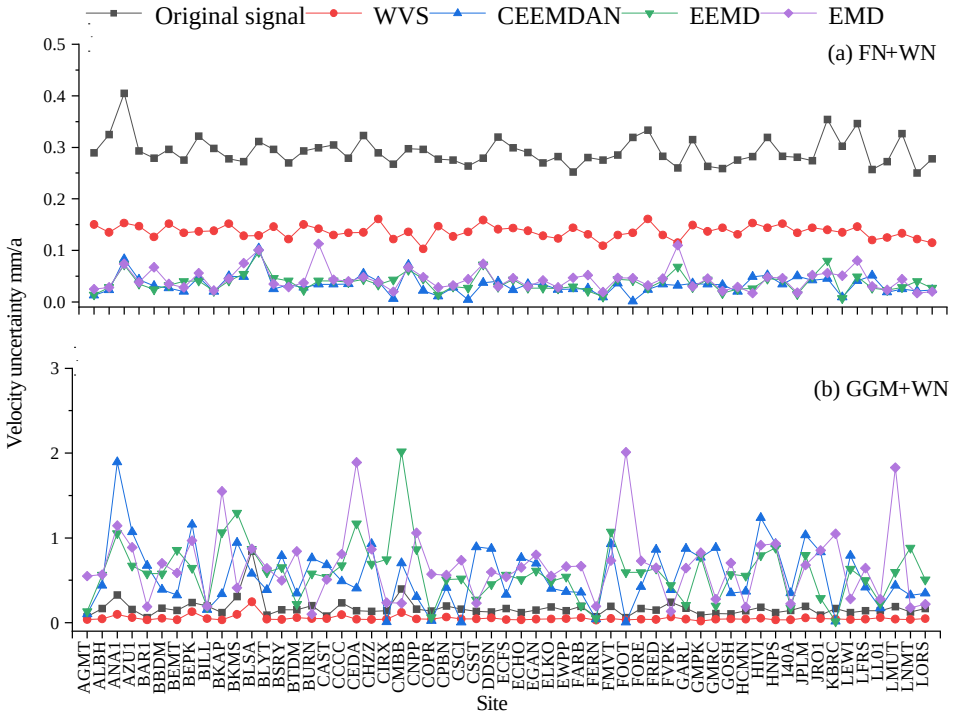

Fig. 10 Comparison results of velocity uncertainty under FNWN and GGMWN noise models after denoising.

As shown in Figures 10 with the FNWN model, all four methods effectively reduce the velocity uncertainty. The velocity uncertainty of the WVS method after denoising is on average reduced by about 0.16 mm/a compared to the velocity uncertainty of the original time series, while CEEMDAN, EEMD and EMD are reduced by about 0.26 mm/a, 0.26 mm/a and 0.24 mm/a, respectively. Similarly, to the distribution of velocity uncertainty for the FNWN noise using the simulated data in Figure 7, in the velocity estimated by CEEMDAN, EEMD and EMD after denoising may be overestimated. With the GGMWN noise model, the velocity uncertainty of the WVS method after denoising is on average reduced by about 0.12 mm/a compared to the velocity uncertainty of the original time series, while CEEMDAN, EEMD and EMD are increased by about 0.39 mm/a, 0.42 mm/a, 0.47 mm/a, respectively. The fact that the velocity uncertainty of the WVS method is reduced and the velocity uncertainty of the other methods is increased shows that the WVS method is more reliable in removing GGMWN noise. It can lead to accurate station velocity values. To determine whether the estimated velocity uncertainty values are reliable, the ratio L estimated before and after denoising, is calculated for the WVS and the other three methods. The comparison results are displayed in Figure 11.

In Figure 11, for the FNWN noise model, about 95 % of the sites show an increase in the relative error of the time series after WVS denoising compared to without denoising them. The ratio is smaller compared to the other three denoising methods. For the GGMWN noise model, the relative error L of the time series after WVS denoising increases compared to the original time series, while the other methods show a decrease in the ratio of the denoised time series. The conclusion obtained is the same as that in Figure 8, indicating that the WVS method can effectively identify FNWN and GGMWN noise and extract useful information from the original time series, providing accurate station velocity values in practical applications compared to the other three methods.

4. CONCLUSION

This article addresses issues such as excessive or insufficient decomposition in VMD due to inappropriate choices of the decomposition mode number k and the penalty factor α. We propose a WOA optimization algorithm with envelope entropy as the objective function to improve the VMD decomposition algorithm. We reconstruct the IMFs after VMD decomposition and calculate the evaluation index values to classify high-frequency and low-frequency signals. The improved SSA algorithm using the comprehensive evaluation index is applied to secondary denoising of high-frequency signals. The effectiveness, reliability and applicability of the WVS method are validated using i) simulated time series with FNWN and GGMWN stochastic noise models, and ii) the vertical component of the daily position of the GNSS station for 100 sites located on the US West Coast. The main conclusions are as follows:

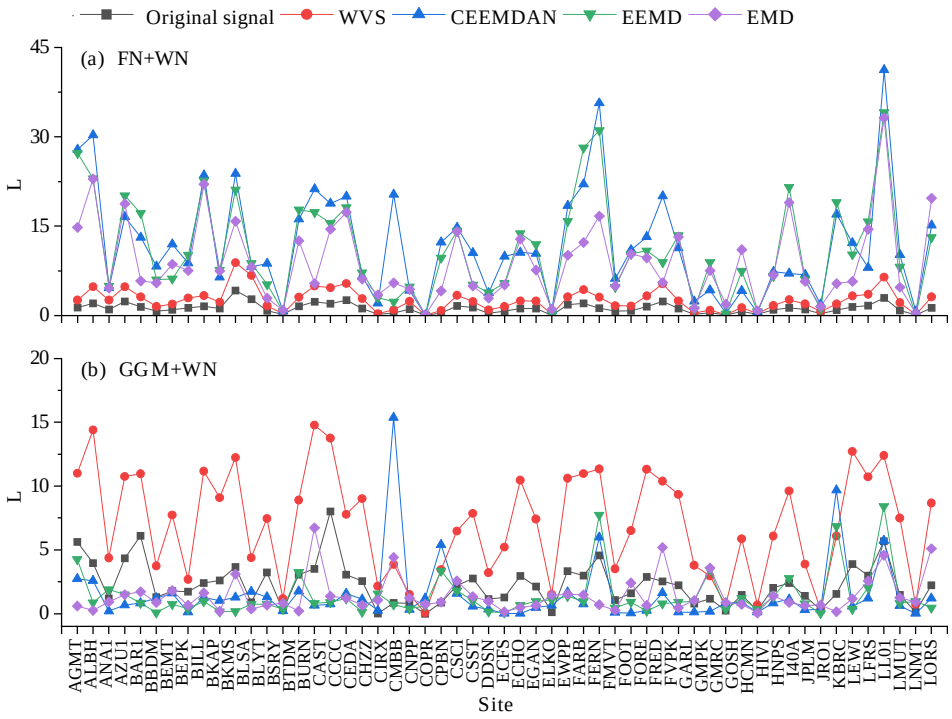

Fig. 11 Result of ratio L under FNWN and GGMWN noise models after site data denoising.

1. An open-source WVS software is designed, which takes advantage of the interactive GUI interface in MATLAB. Classic denoising algorithms such as EMD, EEMD, and CEEMDAN are implemented, as well as the novel WVS denoising algorithm based on VMD, WOA, and SSA. The software also includes functions for time series simulation, data loading, and accuracy evaluation, which together form a complete GNSS time series denoising analysis tool with good interactivity.
2. The experimental results using FNWN and GGMWN stochastic noise models in the simulated time series show that the WVS method, compared to CEEMDAN, EEMD and EMD, reduced the RMSE by an average of about 0.9 mm, increased the SNR and CC by an average of ~1.09 db, ~0.18, respectively. The WVS method is the closest to the true value. We conclude that the algorithm removes better the noise and preserve useful information. The estimated velocity and velocity uncertainty values are the closest to the true values. The denoising process conserve the original time series stochastic noise model and geophysical properties.
3. Using the 100 GNSS station height time series on the US West Coast, we obtain similar results with our new algorithm. It is consistent with the simulation results. After applying the WVS, the station velocity uncertainty is reduced by an average of 0.16 mm/a.

ACKNOWLEDGEMENT

This work was sponsored by National Natural Science Foundation of China (42104023, 42264001), Major Discipline Academic and Technical Leaders Training Program of Jiangxi Province (20225BCJ23014).

The GNSS data is available freely at http://garner.ucsd.edu/pub (WNAM_Clean_TrendNeuTimeSeries_comb_20230501.tar.gz).

REFERENCES

Agnieszka, W. and Dawid, K.: 2022, Modeling seasonal oscillations in GNSS time series with Complementary Ensemble Empirical Mode Decomposition. GPS Solut., 26, 4, 101. DOI: 10.1007/s10291-022-01288-2

Alexandrov, T.: 2008, A method of trend extraction using singular spectrum analysis. arXiv preprint arXiv: 0804.3367. DOI: 10.48550/arXiv.0804.3367

Bertiger, W., Desai, S.D., Haines, B., Harvey, N., Moore, A.W., Owen, S. and Weiss, J.P.: 2010, Single receiver phase ambiguity resolution with GPS data. J. Geod., 84, 5, 327–337. DOI: 10.1007/s00190-010-0371-9

Bock, Y. and Melgar, D.: 2016, Physical applications of GPS geodesy: A review. Rep. Prog. Phys., 79, 10, 106801. DOI: 10.1088/0034-4885/79/10/106801

Bock, Y., Moore, A.W., Argus, D.F., Fang, P., Jiang, S., Kedar S., Knox, S.A., Liu, S.Z. and Sullivan, A.: 2021, Extended Solid Earth Science ESDR System (ES3): Algorithm Theoretical Basis Document, Sept. 19, NASA MEaSUREs project.

Bos, M.S., Fernandes, R.M.S., Williams, S.D.P. and Bastos, L.: 2013, Fast error analysis of continuous GNSS observations with missing data. J. Geod., 87, 4, 351–360. DOI: 10.1007/s00190-012-0605-0

Dey, A., Chhibba, R., Ratnam, D.V. and Sharma, N.: 2021, A combined iCEEMDAN and VMD method for mitigating the impact of ionospheric scintillation on GNSS signals. Acta Geophys., 69, 5, 1933–1948. DOI: 10.1007/s11600-021-00629-y

Dragomiretskiy, K. and Zosso, D.: 2013, Variational mode decomposition. IEEE Trans. Signal Process., 62, 3, 531–544. DOI: 10.1109/TSP.2013.2288675

Elad, M. and Aharon, M.: 2006, Image denoising via sparse and redundant representations over learned dictionaries. IEEE Trans. Image Process., 15, 12, 3736–3745. DOI: 10.1109/TIP.2006.881969

El-Hendawi, M. and Wang, Z.: 2020, An ensemble method of full wavelet packet transform and neural network for short term electrical load forecasting. Electr. Power Syst. Res., 182, 106265. DOI: 10.1016/j.epsr.2020.106265

Fernandes, R.M.S., Ambrosius, B.A.C., Noomen, R., Bastos, L., Combrinck, L., Miranda, J.M. and Spakman, W.: 2004, Angular velocities of Nubia and Somalia from continuous GPS data: implications on present-day relative kinematics. Earth Planet. Sci. Lett., 222, 1, 197–208. DOI: 10.1016/j.epsl.2004.02.008

Han, M., Liu, Y., Xi, J. and Guo, W.: 2006, Noise smoothing for nonlinear time series using wavelet soft threshold. IEEE Signal Process. Lett., 14, 1, 62–65. DOI: 10.1109/LSP.2006.881518

Hassani, H., Mahmoudvand, R. and Zokaei, M.: 2011, Separability and window length in singular spectrum analysis. Comptes Rendus Math., 349, 17–18, 987–990. DOI: 10.1016/j.crma.2011.07.012

He, X., Montillet, J.P., Fernandes, R., Bos, M., Yu, K., Hua, X. and Jiang, W.: 2017, Review of current GPS methodologies for producing accurate time series and their error sources. J. Geodyn., 106, 12–29. DOI: 10.1016/j.jog.2017.01.004

He, X., Yu, K., Montillet, J.P., Xiong, C., Lu, T., Zhou, S., Ma, X., Cui, H. and Ming, F.: 2020, GNSS-TS-NRS: An Open-source MATLAB-Based GNSS time series noise reduction software. Remote Sens., 12, 21, 3532. DOI: 10.3390/rs12213532

Huang, N.E., Shen, Z., Long, S.R., Wu, M.C., Shih, H.H., Zheng, Q., Yen, N.C., Tung, C.C. and Liu, H.H.: 1998, The empirical mode decomposition and the Hilbert spectrum for nonlinear and non-stationary time series analysis. Proc. R. Soc. Lond. A: Math. Phys. Eng. Sci., 454, 1971, 903–995. DOI: 10.1098/rspa.1998.0193

Humphrey, W., Dalke, A. and Schulten, K.: 1996, VMD: visual molecular dynamics. J. Mol. Graph., 14, 1, 33–38. DOI: 10.1016/0263-7855(96)00018-5

Jiang, H., Li, C. and Li, H.: 2013, An improved EEMD with multiwavelet packet for rotating machinery multi-fault diagnosis. Mech. Syst. Signal Process., 36, 2, 225–239. DOI: 10.1016/j.ymssp.2012.12.010

Jin, Z., Chen, G. and Yang, Z.: 2022, Rolling bearing fault diagnosis based on WOA-VMD-MPE and MPSO-LSSVM. Entropy, 24, 7, 927. DOI: 10.3390/e24070927

Lei, Y., He, Z. and Zi, Y.: 2009, Application of the EEMD method to rotor fault diagnosis of rotating machinery. Mech. Syst. Signal Process., 23, 4, 1327–1338. DOI: 10.1016/j.ymssp.2008.11.005

Li, J., Liu, C., Zeng, Z. and Chen, L.: 2015, GPR signal denoising and target extraction with the CEEMD method. IEEE Geosci. Remote Sens. Lett., 12, 8, 1615–1619. DOI: 10.1109/LGRS.2015.2415736

Liu, F., Gao, J. and Liu, H.: 2020, The feature extraction and diagnosis of rolling bearing based on CEEMD and LDWPSO-PNN. IEEE Access, 8, 19810–19819. DOI: 10.1109/ACCESS.2020.2968843

Meinhold, R.J. and Singpurwalla, N.D.: 1983, Understanding the Kalman filter. Am. Stat., 37, 2, 123–127. DOI: 10.2307/2682319

Mirjalili, S. and Lewis, A.: 2016, The whale optimization algorithm. Adv. Eng. Soft., 95, 51–67. DOI: 10.1016/j.advengsoft.2016.01.008

Montillet, J.P., Tregoning, P., McClusky, S. and Yu, K.: 2012, Extracting white noise statistics in GPS coordinate time series. IEEE Geosci. Remote Sens. Lett., 10, 3, 563–567. DOI: 10.1109/LGRS.2012.2213576

Montillet, J.P., Williams, S.D.P., Koulali, A. and McClusky, S.C.: 2015, Estimation of offsets in GPS time-series and application to the detection of earthquake deformation in the far-field. Geophys. J. Int., 200, 2, 1207–1221. DOI: 10.1093/gji/ggu473

Mosavi, M.R., Rezaei, M.J., Pashaian, M. and Moghaddasi, M.S.: 2017, A fast and accurate anti-jamming system based on wavelet packet transform for GPS receivers. GPS Solut., 21, 415–426. DOI: 10.1007/s10291-016-0535-z

Serpelloni, E., Faccenna, C., Spada, G., Dong, D. and Williams, S.D.: 2013, Vertical GPS ground motion rates in the Euro-Mediterranean region: New evidence of velocity gradients at different spatial scales along the Nubia-Eurasia plate boundary. J. Geophys. Res., Solid Earth, 118, 11, 6003–6024. DOI: 10.1002/2013JB010102,2013

Shen, N., Chen, L., Liu, J., Wang, L., Tao, T., Wu, D. and Chen, R.: 2019, A review of global navigation satellite system (GNSS) - based dynamic monitoring technologies for structural health monitoring. Remote Sens., 11, 9, 1001. DOI: 10.3390/rs11091001

Tregoning, P. and Watson, C.: 2009, Atmospheric effects and spurious signals in GPS analyses. J. Geophys. Res., Solid Earth, 114, B9. DOI: 10.1029/2009JB006344

Vautard, R., Yiou, P. and Ghil, M. : 1992, Singular-spectrum analysis: A toolkit for short, noisy chaotic signals. Phys. D: Nonlinear Phenom., 58, 1-4, 95–126. DOI: 10.1016/0167-2789(92)90103-T

Wang, J., Nie, G., Gao, S., Wu, S., Li, H. and Ren, X.: 2021, Landslide deformation prediction based on a GNSS time series analysis and recurrent neural network model. Remote Sens., 13, 6, 1055. DOI: 10.3390/rs13061055

Wang, W.C., Chau, K.W., Xu, D.M. and Chen, X.Y.: 2015, Improving forecasting accuracy of annual runoff time series using ARIMA based on EEMD decomposition. Water Resour. Manag., 29, 2655–2675. DOI: 10.1007/s11269-015-0962-6

Williams, S.D., Bock, Y., Fang, P., Jamason, P., Nikolaidis, R.M., Prawirodirdjo, L., Miller, M. and Johnson, D. J.: 2004, Error analysis of continuous GPS position time series. J. Geophys. Res., Solid Earth., 109, B3. DOI: 10.1029/2003JB002741

Wu, Z., Huang, N.E. and Chen, X.: 2009, The multi-dimensional ensemble empirical mode decomposition method. Adv. Adapt. Data Anal., 1, 3, 339–372. DOI: 7sup.top/10.1142/S1793536909000187

Xiao, M., Zhang, C., Wen, K., Xiong, L., Geng, G. and Wu, D.: 2018, Bearing fault feature extraction method based on complete ensemble empirical mode decomposition with adaptive noise. J. Vibroeng., 20, 7, 2622–2631. DOI: 10.21595/jve.2018.19562

Xiong, C., Yu, L. and Niu, Y.: 2019, Dynamic parameter identification of a long-span arch bridge based on GNSS-RTK combined with CEEMDAN-WP analysis. Appl. Sci., 9, 7, 1301. DOI: 10.3390/app9071301

Xu, H., Lu, T., Montillet, J.P. and He, X.: 2021, An improved adaptive IVMD-WPT-Based noise reduction algorithm on GPS height time series. Sensors, 21, 24, 8295. DOI: 10.3390/s21248295

Yen, G.G. and Lin, K.C.: 2000, Wavelet packet feature extraction for vibration monitoring. IEEE Trans. Ind. Electron., 47, 3, 650–667. DOI: 10.1109/41.847906

Zhang, R., Gao, C., Pan, S. and Shang, R.: 2020, Fusion of GNSS and speedometer based on VMD and its application in bridge deformation monitoring. Sensors, 20, 3, 694. DOI: 10.3390/s20030694

Zhang, X., Miao, Q., Zhang, H. and Wang, L.: 2018, A parameter-adaptive VMD method based on grasshopper optimization algorithm to analyze vibration signals from rotating machinery. Mech. Syst. Signal Process., 108, 58–72. DOI: 10.1016/j.ymssp.2017.11.029

Zumberge, J.F., Heflin, M.B., Jefferson, D.C., Watkins, M.M. and Webb, F. H.: 1997, Precise point positioning for the efficient and robust analysis of GPS data from large networks. J. Geophys. Res., Solid Earth, 102, B3, 5005–5017. DOI: 10.1029/96JB03860